

Signature of Magnetic Phase Separation in the Ground State of $\text{Pr}_{1-x}\text{Ca}_x\text{MnO}_3$

Hao Sha,¹ F. Ye,² Pengcheng Dai,^{3,2} J. A. Fernandez-Baca,^{2,3} D. Mesa,¹
J. W. Lynn,⁴ Y. Tomioka,⁵ Y. Tokura,^{5,6} and Jiandi Zhang^{1,*}

¹*Department of Physics, Florida International University, Miami, Florida 33199*

²*Neutron Scattering Science Division, Oak Ridge National Laboratory, Oak Ridge, Tennessee 37831-6393*

³*Department of Physics and Astronomy, The University of Tennessee, Knoxville, Tennessee 37996-1200*

⁴*NIST Center for Neutron Research, Gaithersburg, Maryland, 20899-6102*

⁵*Correlated Electron Research Center (CERC), National Institute of Advanced Industrial Science and Technology (AIST), Tsukuba 305-0046, Japan*

⁶*Department of Applied Physics, University of Tokyo, Tokyo 113-8656, Japan*

(Dated: October 24, 2018)

Neutron scattering has been used to investigate the evolution of the long- and short-range charge-ordered (CO), ferromagnetic (FM), and antiferromagnetic (AF) correlations in single crystals of $\text{Pr}_{1-x}\text{Ca}_x\text{MnO}_3$. The existence and population of spin clusters as reflected by short-range correlations are found to drastically depend on the doping (x) and temperature (T). Concentrated spin clusters coexist with long-range canted AF order in a wide temperature range in $x = 0.3$ while clusters do not appear in $x = 0.4$ crystal. In contrast, both CO and AF order parameters in the $x = 0.35$ crystal show a precipitous decrease below ~ 35 K where spin clusters form. These results provide direct evidence of magnetic phase separation and indicate that there is a critical doping x_c (close to $x = 0.35$) that divides the phase-separated site-centered from the homogeneous bond-centered or charge-disproportionated CO ground state.

PACS numbers: 75.47.Lx, 61.05.F-, 72.15.Gd

The $R_{1-x}A_x\text{MnO}_3$ (where R and A are rare- and alkaline-earth ions) manganites, known for the existence of “colossal” magnetoresistance, provide an archetype laboratory for the study of phase inhomogeneities [1]. In general, doping (x) not only causes a quenched disorder due to the size mismatch of A -site cations in the perovskite lattice, but also induces a distinctive chemical valence in Mn ions (Mn^{3+} vs. Mn^{4+} in the original portrayal [2, 3]). These two kinds of Mn ions can assemble themselves into a CE-type checkerboard-like charge ordered (CO) state at low temperature (LT) as shown in Fig. 1(b), promoting an antiferromagnetic (AF) insulating phase that competes with the ferromagnetic (FM) metallic state [4, 5, 6]. In a conventional CO state, referred to as a site-centered CO structure, distinct Mn^{3+} and Mn^{4+} ions in half-doped manganites ($x = 0.5$) form 1:1 ratio. However, another possible CO pattern may also occur, namely the bond-centered structure in which the charge is localized not on Mn sites but on Mn-O-Mn bonds with no distinctive $\text{Mn}^{3+}/\text{Mn}^{4+}$ sites [7, 8, 9, 10], thus raising an unsettled issue about the nature of the ground state around $x = 0.5$.

Furthermore, even in some non half-doped ($x \neq 0.5$) manganites, an ostensible *pseudo*-CE-type CO state has been reported [6, 12, 13, 14]. Within the CE-type CO frame, excess of electronic charge (or Mn^{3+} ions) with respect to the ideal half-doped ($x = 0.5$) case exists in these non half-doped compounds. Consequently, important issues naturally emerge: how is the excessive electronic charge distributed in the CO state and what are the arrangements of spins and orbitals? There are at least three possible scenarios based on the charge distribution.

First, the excessive electronic charge is distributed locally in the CE-type motif with distinct Mn^{3+} and Mn^{4+} sites. Apparently an electronic/magnetic phase separation is unavoidable due to unequal amount of Mn^{3+} and Mn^{4+} ions while keeping the rigid CE-type Mn^{3+} and Mn^{4+} order. Another one is that the excessive charge is distributed uniformly in the CE-type motif with certain charge disproportionation (δ) [15, 16]. Both scenarios can be categorized as the site-centered structure because of having distinctive Mn sites, one inhomogeneous while the other homogeneous. The third scenario is the completely homogenous bond-centered structure in which all Mn sites are equivalent ($\delta = 0$) [7, 17]. Presently it is unclear which scenario is more appropriate for the observed CO state. Alternatively, could it be possible that the CO structure depends on doping concentration?

In this letter, we report the signature of magnetic phase separation in the CO state from neutron scattering studies of a prototype manganite system: $\text{Pr}_{1-x}\text{Ca}_x\text{MnO}_3$ (PCMO). Our experimental results suggest a critical doping concentration x_c that divides homogeneous and inhomogeneous CO ground state. As shown in Fig. 1 (a), the non-metallic CO ground state of PCMO exists over a broad doping range ($0.3 \leq x \leq 0.7$) [6]. Because Pr^{3+} and Ca^{2+} have almost equal ion radii, PCMO has negligible quenched disorder, and thus is an ideal system to elucidate how doping affects the structure of CO and magnetic ground states.

Three single crystals with $x = 0.3$ (PCMO30), 0.35 (PCMO35), and 0.4 (PCMO40) were grown by the floating-zone method [6]. The measurements were carried out using the HB-1 and HB-3 triple-axis spectrom-

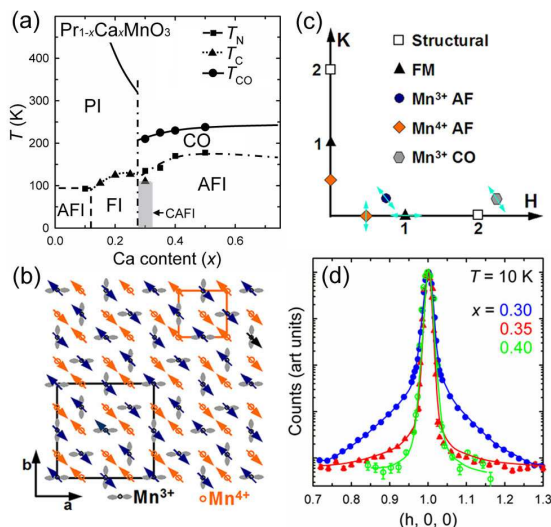


FIG. 1: (a) Generic phase diagram of $\text{Pr}_{1-x}\text{Ca}_x\text{MnO}_3$ [6]. (b) Schematic ab -plane view of the CE-type structure with both orbital ($d_{3x^2-r^2}/d_{3y^2-r^2}$) and spin ordering. The bigger square denotes the Mn^{3+} orbital/magnetic unit cell while the smaller square shows the Mn^{4+} magnetic unit cell. (c) The probed superlattice peak positions and the scan directions (marked by arrows) in reciprocal space. (d) Normalized q -scan profiles of the scattering near $(1, 0, 0)$ at $T = 10$ K for PCMO30 (blue), PCMO35 (red), and PCMO40 (green). The solid lines are guides to the eye.

eters at the High Flux Isotope Reactor at the Oak Ridge National Laboratory (ORNL), BT-7, and BT-9 at the NIST Center for Neutron Research. For simplicity, we label all wave vectors in terms of the pseudocubic unit cell with lattice parameters of $a = 3.87$ Å, although all of our samples have orthorhombic structures slightly distorted from the cubic lattice. The wave vector $\mathbf{Q} = (Q_x, Q_y, Q_z)$ is in the unit of Å⁻¹ and $(H, K, L) = (Q_x a / 2\pi, Q_y a / 2\pi, Q_z a / 2\pi)$ is in reciprocal lattice units (rlu). The samples were aligned to allow the wave vector in the form of $(H, K, 0)$ accessible in the horizontal scattering plane.

All of the measurements were based upon the CE-type structure with CO and AF ordering shown in Fig. 1(b). Including the orbital part, the periodicity of AF order for Mn^{3+} spins is twice of that for Mn^{4+} spins. As shown in Fig. 1(c)[18], we used $\mathbf{Q} = (2.25, 0.25, 0)$, $(1, 0, 0)$, $(0.75, 0.25, 0)$, and $(0.5, 0, 0)$, to probe the order of the CO, FM, AF at Mn^{3+} and Mn^{4+} sites, respectively. The corresponding short-range correlations or, alternatively, clusters, were also determined by measuring the diffuse scattering around these characteristic positions [19]. As listed in Table 1, the measured transition temperatures for CO, AF, and FM phase are in agreement with those reported in the literature. A canted long-range FM order coexists with an AF structure in PCMO30 below $T_C = 110$ K (see the inset (a) of Fig. 2), known as a canted AF

insulating (CAFI) phase [20]. However, no long-range FM order was detected in the ground state for either PCMO35 or PCMO40.

$\text{Pr}_{1-x}\text{Ca}_x\text{MnO}_3$	$x = 0.30$	$x = 0.35$	$x = 0.40$
$T_{CO}; T_N; T_C$ (K)	210;125;110	230;160;N/A	245;170;N/A
$\rho_{FM} (\times 100\%)$	15.1 ± 2.0	N/A	N/A
$\rho_{AF} (\times 100\%)$	28.7 ± 0.8	0.160 ± 0.003	N/A

TABLE I: The integrated intensity ratios of the diffuse and total (diffuse plus Bragg) magnetic scattering ($\rho_{FM,AF} \equiv I_{diffuse}(FM, AF)/I_{total}(FM, AF)$) vs. x measured at 10 K: ρ_{FM} , the ratio obtained from the scan across $(1, 0, 0)$ by subtracting the lattice contribution to the Bragg peak; ρ_{AF} , the ratio obtained from the scan across $(0.5, 0, 0)$.

We observed a strong doping dependence of both AF and FM diffuse scattering at the ground state. Figure 1(d) displays the normalized q -scans at $(1, 0, 0)$ including both magnetic and structural scattering from the three doping levels. Similar to that reported before [20, 21], a strong diffuse component appears near the Bragg peak for PCMO30, which indicates that FM spin clusters coexist with the long-range FM order in the ground state. In contrast, PCMO35 has a rather weak FM diffuse shoulder. PCMO40 shows only a nice Gaussian profile due to long-range lattice scattering with no sign of short-range spin correlation. The AF scattering profiles at $(0.5, 0, 0)$ and $(0.75, 0.25, 0)$ reveal a similar x -dependence of diffuse components. As summarized in Table 1, PCMO30 has a CAFI ground state with a significant amount of FM/AF clusters ($\rho_{FM} \approx 15.1 \pm 2.0\%$ and $\rho_{AF} \approx 28.7 \pm 0.8\%$). PCMO35 has an almost homogeneous AF ground state with a very small weight of spin clusters, and PCMO40 has a completely uniform AF ground state. Therefore, a critical doping x_c must exist and be very close to the value of $x = 0.35$, which serves as the boundary between the homogeneous and inhomogeneous ground state of $\text{Pr}_{1-x}\text{Ca}_x\text{MnO}_3$.

To further reveal such a critical doping behavior for the inhomogeneity in the magnetic structure, we have examined the T -dependence of the FM diffuse scattering intensity at $\mathbf{Q} = (0.96, 0, 0)$, which is outside the influence of the Bragg peak for long-range ordering. Figure 2 presents the measured intensity as a function of T/T_{CO} for all three doping levels. Similar behavior is obtained for different positions (see the inset (b) of Fig. 2). The FM diffuse component clearly displays a different T -dependence above and below T_{CO} . Comparable results have also been reported by Kajimoto *et al.* [21]. When $T > T_{CO}$, all three doping levels of crystals exhibit a similar T -dependence of the diffuse component, reflecting the FM spin fluctuations in the paramagnetic phase, which are presumably induced by double-exchange (DE) interaction [1].

On the other hand, a completely different T -

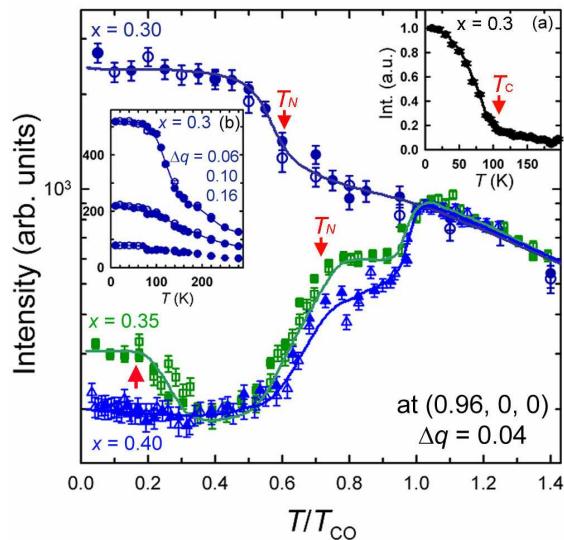


FIG. 2: T -dependence of the FM diffuse component measured at $(0.96, 0, 0)$ ($\Delta q = 0.04$ rlu) for different x 's of $\text{Pr}_{1-x}\text{Ca}_x\text{MnO}_3$ on cooling (solid symbols) and warming (open symbols). The solid curves are guides to the eye. Arrows mark the Curie and Néel temperatures, as well as the onset of spin phase separation for PCMO35. The insets present the T -dependence of (a) the FM order parameter (Bragg peak intensity) and (b) the FM diffuse component at selected q positions from $(1, 0, 0)$ for PCMO30.

dependence of the diffuse components for different doping levels appears below T_{CO} . For PCMO40, the FM spin fluctuations deteriorate below T_{CO} and vanish below T_N . In principle, such a T -dependence in PCMO40 can be understood as follows. When $T < T_{CO}$, the DE-mediated FM spin fluctuations will be suppressed by the charge localization. When $T < T_N$, the FM fluctuations diminish further because of the onset of AF order. For PCMO35, the FM spin fluctuations exhibit the same T -dependence as those in PCMO40, thus indicating that they originate from the same mechanism. However, spin clusters appear below ~ 65 K with both FM (see Fig. 2) and AF characters, as reflected by the corresponding diffuse components. This is distinctive from the FM spin fluctuations at high temperature. In sharp contrast with those in both PCMO35 and PCMO40, the population of spin clusters in PCMO30, reflected by the intensity of FM diffuse component, increases rather than decreases below T_{CO} . Surprisingly, it increases much more drastically below T_N , regardless of the establishment of AF order, thus suggesting the spin clusters in the ground state may have a different nature from the DE-mediated FM fluctuations at high temperature.

The spin clusters appearing in PCMO30 in the LT regime also display both FM and AF characters, similar to those existing in the ground state of PCMO35. The integrated diffuse scattering intensity and the extracted short-range correlation length ξ near the FM and

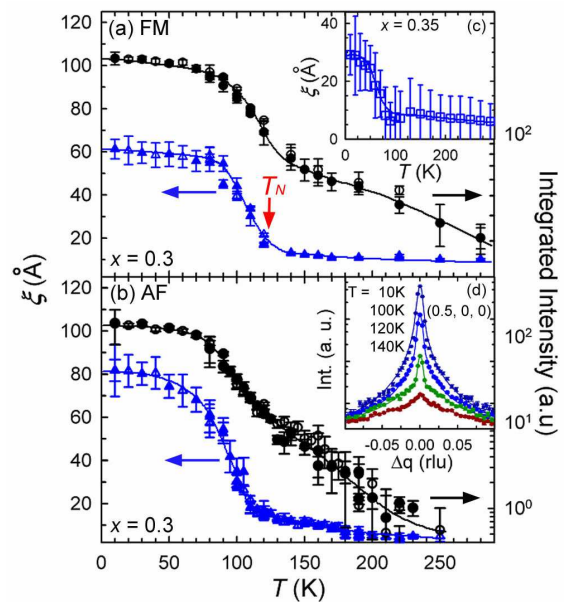


FIG. 3: T -dependence of the intensity and extracted short-range correlation length of (a) FM at $(1, 0, 0)$ and (b) Mn^{4+} AF at $(0.5, 0, 0)$ in PCMO30. The solid lines are guides to the eye. The solid symbols are for cooling while open symbols for warming. The insets show the T -dependence of (c) FM short-range correlation length in PCMO35 with large error bars due to the weak diffuse scattering profiles and (d) q -scans of Mn^{4+} AF at $(0.5, 0, 0)$.

AF peak exhibit very similar T -dependence (see Fig. 3). The measured average cluster diameter (*i.e.* correlation length) is $\xi_{FM} \approx 60$ Å from FM and $\xi_{AF} \approx 80$ Å from AF scattering. Using a simple estimated population relation in the ab -plane of the crystal: $\rho_{FM,AF} \propto n_{FM,AF} \xi_{FM,AF}^2$, where $n_{FM,AF}$ is the in-plane cluster density, we find that $n_{FM} \cong n_{AF}$ with measured $\rho_{FM,AF}$ (Table 1), regardless of the difference in correlation length. Therefore, we speculate that the measured AF and FM diffuse scattering may be indeed caused from the same assembly of spin clusters.

Due to the fairly weak diffuse scattering and uncertain correlation length (see the inset (c) of Fig. 3) we were not able to do a similar estimation for PCMO35. Nevertheless, the ground state in both PCMO30 and PCMO35 is a phase-separated state containing spin clusters embedded in either an AF or canted AF ordered matrix. The main difference between these two doping levels is that the magnetic phase separation exists in the entire measured temperature range in PCMO30 but appears with much smaller population only at LT in PCMO35. One can anticipate that such a phase-separated ground state will disappear in a crystal of $\text{Pr}_{1-x}\text{Ca}_x\text{MnO}_3$ with a doping level slightly larger than $x = 0.35$. Such an evolution of phase separation with doping may provide insight into the doping dependence of the observed CMR effect [6]. This evolution may also explain why a smaller

critical magnetic field is sufficient to melt the CO state for PCMO30 than that for PCMO35 and PCMO40.

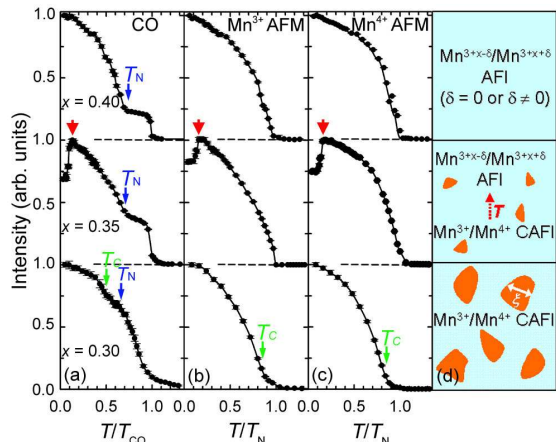


FIG. 4: T -dependence of order parameters for (a) CO structure measured at (2.25, 0.25, 0), (b) Mn^{3+} AF ordering at (0.75, 0.25, 0), and (c) Mn^{4+} AF ordering at (0.5, 0, 0), for the three doping x 's of $\text{Pr}_{1-x}\text{Ca}_x\text{MnO}_3$. Arrows mark the Curie and Néel temperatures as well as the onset of phase separation for PCMO35. The column (d) illustrates the evolution from an inhomogeneous site-centered to a homogeneous CO phase for corresponding doping levels.

If indeed PCMO35 is a system which undergoes a phase evolution from homogeneous to inhomogeneous spin-ordered state on cooling, then the appearance of spin clusters at LT should affect the long-range order parameters. To elucidate this issue we have investigated systematically the order parameters of the CO and AF at both Mn^{3+} and Mn^{4+} sites, respectively. As clearly shown in Fig. 4, an anomaly characterized by a sudden drop in the intensity of the measured order parameters in PCMO35 emerges at ~ 35 K, coinciding with the establishment of spin clusters and thus, providing a clear signature of magnetic phase separation. In addition, we note that the line shape of these order parameters in PCMO30 near both T_{CO} and T_N is slightly different from that in PCMO35 and PCMO40. The transitions in PCMO35 and PCMO40 show more pronounced critical behavior than those in PCMO30. The nature behind this should be associated with the existence of phase separation near T_N and T_{CO} in PCMO30, which does not occur in the other two doping levels.

In summary, we have observed a strong x - and T -dependence of magnetic phase separation in $\text{Pr}_{1-x}\text{Ca}_x\text{MnO}_3$ crystals. Spin clusters with both AF and FM correlations coexist with a CAFI structure in PCMO30, suggesting an inhomogeneous CO state below T_{CO} . The ground state of PCMO30 is inhomogeneous site-centered ($\delta > 0$) or even in the extreme case, the inhomogeneous CE-type [see Fig. 4(d)]. In contrast, the observed uniform AF ordered structure suggests a homogeneous AF CO state in PCMO40. We have identified a

critical doping x_c , which is very close to $x = 0.35$, to divide homogeneous and inhomogeneous CO ground states. Whether the homogenous CO state exists in PCMO40 as a site-centered type with charge disproportionation ($\delta \neq 0$) or a bond-centered type is still unclear. One possible experimental method to distinguish these two types of CO structures is resonant x-ray scattering [22]. Yet, it is clear that in a manganite away from half doping, a CE-type $\text{Mn}^{3+}/\text{Mn}^{4+}$ CO state can not survive without phase separation.

This work was supported by U.S. DOE FG02-o4ER46125 and NSF DMR-0346826. P.D. was supported by U.S. NSF DMR-0756568. ORNL is managed by UT-Battelle, LLC, for the U.S. DOE DE-AC05-00OR22725.

* Electronic address: zhangj@fju.edu

- [1] E. Dagotto, *Nanoscale Phase Separation and Colossal Magnetoresistance* (Berlin: Springer, 2002); *Science* **309**, 257 (2005).
- [2] E.O. Wollan and W.C. Koehler, *Phys. Rev.* **100**, 545 (1955).
- [3] J.B. Goodenough, *Phys. Rev.* **100**, 564 (1955).
- [4] Z. Jirák *et al.*, *J. Magn. Magn. Mater* **15-18**, 519 (1980).
- [5] Y. Tokura *et al.*, *Phys. Rev. Lett.* **76**, 3184 (1996); Y. Tokura and N. Nagaosa, *Science* **288**, 462 (2000).
- [6] Y. Tomioka *et al.*, *Phys. Rev. B* **53**, R1689 (1996).
- [7] A. Daoud-Aladine *et al.*, *Phys. Rev. Lett.* **89**, 97205 (2002).
- [8] V. Ferrari *et al.*, *Phys. Rev. Lett.* **91**, 227202 (2003).
- [9] G. Zheng and C. H. Patterson, *Phys. Rev. B* **67**, 220404 (2002).
- [10] C. Zener, *Phys. Rev.* **82**, 403 (1951); J.-S. Zhou and J.B. Goodenough, *Phys. Rev. B* **62**, 3834 (2000).
- [11] D. V. Efremov *et al.*, *Nature Materials* **3**, 853 (2004).
- [12] E. Pollert *et al.*, *J. Phys. Chem. Solids* **43**, 1137 (1982).
- [13] T. Asaka *et al.*, *Phys. Rev. Lett.* **88**, 097201 (2002); Y. Tokura, *Prog. Rep. Phys.* **69**, 797 (2006).
- [14] D.E. Cox *et al.*, *Phys. Rev. B* **57**, 3305 (1998); M. v. Zimmermann *et al.*, *Phys. Rev. B* **64**, 195133 (2001).
- [15] J. van den Brink *et al.*, *Phys. Rev. Lett.* **83**, 5118 (1999); Z. Popović and S. Satpathy, *Phys. Rev. Lett.* **88**, 197201 (2002).
- [16] S. Grenier *et al.*, *Phys. Rev. B* **69**, 134419 (2004).
- [17] Ch. Jooss *et al.*, *Proc. Natl. Acad. Sci. U.S.A.* **104**, 13597 (2007).
- [18] F. Ye *et al.*, *Phys. Rev. B* **72**, 212404 (2005).
- [19] The diffuse components of scattering were fitted to Lorentzian lineshapes convoluted with the instrumental resolution. The linewidth Γ corresponds to the inverse correlation length ($\Gamma = 1/\xi$), where ξ is also the spin cluster size. The intensity of the Lorentzians is proportional to the population of spin clusters.
- [20] H. Yoshizawa *et al.*, *Phys. Rev. B* **52**, R13145 (1995); P. G. Radaelli *et al.*, *Phys. Rev. B* **63**, 172419 (2001); J.A. Fernandez-Baca *et al.*, *Phys. Rev. B* **66**, 054434 (2002).
- [21] R. Kajimoto *et al.*, *Phys. Rev. B* **58**, R11837 (1998).
- [22] P. Abbamonte, *Phys. Rev. B* **74**, 195113 (2006).